PNAS RESEARCH ARTICLE | NEUROSCIENCE

Pain hypersensitivity in a pharmacological mouse model of attention-deficit/hyperactivity disorder

Otmane Bouchatta[a,b,1], Franck Aby[c], Wahiba Sifeddine[b], Rabia Bouali-Benazzouz[c], Louison Brochoire[c], Houria Manouze[b], Pascal Fossat[c], Saadia Ba M'Hamed[b], Mohamed Bennis[b,2], and Marc Landry[c,d,2,3]

Edited by Donald Pfaff, Rockefeller University, New York, NY; received August 27, 2021; accepted May 13, 2022

Clinical evidence suggests that pain hypersensitivity develops in patients with attention-deficit/hyperactivity disorder (ADHD). However, the mechanisms and neural circuits involved in these interactions remain unknown because of the paucity of studies in animal models. We previously validated a mouse model of ADHD obtained by neonatal 6-hydroxydopamine (6-OHDA) injection. Here, we have demonstrated that 6-OHDA mice exhibit a marked sensitization to thermal and mechanical stimuli, suggesting that phenotypes associated with ADHD include increased nociception. Moreover, sensitization to pathological inflammatory stimulus is amplified in 6-OHDA mice as compared to shams. In this ADHD model, spinal dorsal horn neuron hyperexcitability was observed. Furthermore, ADHD-related hyperactivity and anxiety, but not inattention and impulsivity, are worsened in persistent inflammatory conditions. By combining in vivo electrophysiology, optogenetics, and behavioral analyses, we demonstrated that anterior cingulate cortex (ACC) hyperactivity alters the ACC–posterior insula circuit and triggers changes in spinal networks that underlie nociceptive sensitization. Altogether, our results point to shared mechanisms underlying the comorbidity between ADHD and nociceptive sensitization. This interaction reinforces nociceptive sensitization and hyperactivity, suggesting that overlapping ACC circuits may be targeted to develop better treatments.

attention-deficit/hyperactivity disorder | pain sensitization | comorbidity | anterior cingulate cortex | spinal cord

Significance

Attention-deficit/hyperactivity disorder (ADHD) is a neurodevelopmental disorder that often exhibits comorbid alterations in sensitivity. Patients with ADHD report sensitization to pain, but no data exist on the mechanisms involved. We used a validated mouse model to characterize nociceptive sensitization to peripheral stimuli in ADHD-like conditions, and to demonstrate that this sensitization is further amplified in a pathological inflammatory state. We provide functional evidence that nociceptive sensitization relies on top-down circuits that originate in the cortex and modify nociceptive spinal networks. Our data indicate that ADHD and persistent pain are mutually worsening comorbid disorders with reciprocal worsening of nociceptive sensitization and hyperactivity, and new treatments should target overlapping mechanisms for better efficiency.

Attention-deficit/hyperactivity disorder (ADHD) is a common neurodevelopmental disorder associated with cognitive, emotional, and behavioral deficits (1). It is one of the most common psychiatric pathologies in children, with an estimated prevalence of 8 to 12% worldwide (2). Hyperactivity, inattention, and impulsivity (3) are ADHD core symptoms that persist into adulthood in up to two-thirds of patients (4). Patients with ADHD also often have coexisting complaints such as social disabilities and emotional deficits (5).

Individuals who retain greater symptomatology are likely to exhibit psychiatric comorbidity (6, 7). Recent studies indicate an association between attention deficits and altered sensory processing (8). Attentional processes have been shown to regulate pain transmission through the modulation of brain networks (9) and descending pathways (10). In clinical consultations, patients with ADHD report increased pain perception (11–14). Studies suggested that adults with ADHD have an increased risk of pain disorder (15) and are more likely to have taken pain medication in the past years (16). Conversely, chronic pain causes cognitive impairments and worsens ADHD symptoms in human (17–19) and animal models (20).

Despite this body of evidence indicating comorbidity, investigations of ADHD and pain are mostly conducted separately. Few studies have explored the mechanisms and neural systems underlying interactions between ADHD and pain (21, 22), but more knowledge is key to developing better treatments. Therefore, the effects of ADHD on pain transmission and the brain circuits involved need to be further clarified.

The role of dopamine dysregulation in the etiology of ADHD has been highlighted in human and animal models of ADHD (23–25). A loss of dopaminergic signaling is implicated in the symptoms of ADHD hyperactivity (26), and anatomic-functional changes have been demonstrated in dopamine-related areas, particularly in the prefrontal, including the anterior cingulate cortex (27, 28). Among the treatments used to combat ADHD, atomoxetine and methylphenidate (Mph) block the noradrenaline and dopamine transporters, respectively. Accordingly, we previously validated an ADHD mouse model generated at P5 by the disruption of the central dopaminergic pathways with 6-hydroxydopamine (6-OHDA) with good face, predictive, and construct validity (29, 30). Here, we use this well-validated model to address the interplay between ADHD-like conditions and nociception.

Author contributions: O.B., S.B.M., M.B., and M.L. designed research; O.B., F.A., W.S., R.B.-B., L.B., H.M., and M.L. performed research; O.B., P.F., and M.L. analyzed data; O.B., M.B., and M.L. wrote the paper; and R.B.-B, P.F., S.B.M, M.B., and M.L. student supervision.

The authors declare no competing interest.

This article is a PNAS Direct Submission.

[1]Present address: Department of Clinical and Experimental Medicine, Center for Social and Affective Neuroscience, Linköping University, Sweden.

[2]M.B. and M.L. contributed equally to this work.

[3]To whom correspondence may be addressed. Email: marc.landry@u-bordeaux.fr.

This article contains supporting information online at http://www.pnas.org/lookup/suppl/doi:10.1073/pnas.2114094119/-/DCSupplemental.

Published July 19, 2022.

Our data provide clear evidence for increased sensitivity to various nociceptive modalities in 6-OHDA mice and point to circuits that may be impaired in ADHD-like conditions. Altogether, the present results indicate that ADHD and persistent pain are comorbid disorders with mutually worsening adverse effects on nociceptive sensitization and hyperactivity.

Results

ADHD-Like Conditions Influence Sensitivity to Inflammatory Stimulus. We analyzed nociceptive behavioral responses to thermal and mechanical stimuli using the hot/cold plate and von Frey tests (Fig. 1 *A*–*C* and Dataset S1). The paw-licking latency appeared significantly shorter in 6-OHDA mice in response to hot and cold stimuli (Fig. 1 *A* and *B*). The von Frey test showed a significant decrease in the mechanical withdrawal threshold in 6-OHDA mice (Fig. 1*C*). This finding indicated that ADHD-like conditions increased basal sensitivity to thermal and mechanical stimuli.

We then investigated whether ADHD-induced nociceptive sensitization was altered in a model of inflammatory pain obtained by Complete Freund's Adjuvant (CFA) injection in sham and 6-OHDA mice (Fig. 1 *D* and *E* and Dataset S1). NaCl injection in the hind paw had no effect on thermal (Fig. 1 *D*, *1* and *2*) and mechanical sensitivity (Fig. 1*D*, *3*) in either group. Sham animals showed a significant decrease in nociceptive thresholds to thermal (Fig. 1 *D*, *1* and *2*) or mechanical (Fig. 1*D*, *3*) stimuli at 4 d post-CFA. Swiss mice thresholds were consistent with those obtained in C57/Bl6 mice in another recent study (31), although they were seemingly higher in Swiss mice than in C57/Bl6 mice due to weight/size differences (32). The 6-OHDA mice exhibited a further decrease in thermal (Fig. 1 *D*, *1* and 2) and mechanical (Fig. 1*D*, *3*) thresholds in inflammatory conditions. Notably, the comparison between groups indicated that in ADHD-like conditions, CFA-induced pain sensitization to thermal (Fig. 1 *E*, *1* and 2) or mechanical (Fig. 1*E*, *3*) stimuli is amplified, suggesting that ADHD-like conditions worsen central sensitization processes.

Next, we explored the capacity of ADHD medication to alter nociception by injecting a single dose of Mph (intraperitoneal, 3.0 or 5.0 mg/kg) (*SI Appendix*, Fig. S1 *A*–*C* and Dataset S2) that decreased hyperactivity as previously reported (29, 30). Neither 3.0 mg/kg nor 5.0 mg/kg Mph influenced the thermal or mechanical sensitivity (*SI Appendix*, Fig. S1 *A*–*C*) of 6-OHDA or sham mice. Similarly, no effect of Mph was seen in the control (NaCl) or inflammatory (CFA) conditions in both groups (sham and 6-OHDA) (*SI Appendix*, Fig. S1 *D*–*I* and Dataset S2). These data indicated that Mph is ineffective on 6-OHDA–induced thermal and mechanical hyperalgesia/allodynia, regardless of the inflammatory status.

We also demonstrated that changes in nociceptive reflexes are not just a consequence of locomotor hyperactivity (*SI Appendix*, Fig. S2 and Dataset S3). We used intraperitoneal injection of ibuprofen, known to alleviate pain-like behaviors in mice (33), but not to trigger any change in locomotor activity. The resulting increase in mechanical sensitization without a change in the locomotor parameters confirmed that nociceptive behavior and hyperactivity are actually uncorrelated.

ADHD-Like Conditions Change Sensory Integration in the Spinal Cord. We performed single-unit in vivo extracellular recording of deep dorsal horn neurons (DHNs) identified as wide dynamic range (WDR) neurons after peripheral electrical stimulation (*SI Appendix*, Fig. S3*A*). First, 6-OHDA mice DHNs responded to an innocuous stimulus (from the 1.4 g von Frey filament) in contrast to sham mice (Fig. 2 *A* and *C*). Second, 6-OHDA mouse DHNs displayed an increased discharge in response to noxious stimuli (Fig. 2 *A* and *C*). Mph did not influence DHN firing in sham and 6-OHDA mice (Fig. 2*C* and *SI Appendix*, Fig. S3*B*). In inflammatory conditions, recordings showed increased DHN activity in response to innocuous and noxious stimuli (Fig. 2 *B* and *C*) in sham mice as compared to controls (NaCl injection). CFA injection caused a further amplification of DHN activity in 6-OHDA mice (Fig. 2 *B* and *C*). Again, no effects of Mph were seen in sham or 6-OHDA mice in inflammatory conditions (Fig. 2*C* and *SI Appendix*, Fig. S3*C* and Dataset S4).

ADHD-Like Conditions Modify Dorsal Spinal Networks. Given the changes in DHN activity, we investigated possible anatomical and biochemical modifications in the dorsal spinal cord (Fig. 3). We characterized the distribution of synaptic markers of inhibitory and excitatory synapses. We assessed the intensity of the immunostaining for postsynaptic gephyrin (Fig. 3*A*) and homer 1 (Fig. 3*B*), respectively, and their colocalization with presynaptic synaptophysin. Gephyrin (Fig. 3 *A*, *a1–f1* and *a2–f2*) and homer 1 (Fig. 3 *B*, *a1–f1* and *a2–f2*) immunostaining appeared as punctate labeling in the superficial and deeper laminae of the dorsal spinal cord, with the highest density in the lamina II. No changes were observed in the inhibitory synapses (Fig. 3*A*). In contrast, immunostaining for homer 1 was stronger in 6-OHDA mice as compared to sham mice (Fig. 3 *B*, *a1–f1* and *a2–f2*). Quantitative assessment confirmed the increased immunolabeling intensity for homer 1 and the enhanced colocalization of the excitatory postsynaptic marker with synaptophysin (Fig. 3*B*). Taken together, these data provide evidence for increased excitatory transmission in the dorsal spinal cord.

In a second step, we indirectly evaluated in adult mice the depletion in catecholamines induced by neonatal 6-OHDA injection by using TH immunodetection in various brain areas (Fig. 3*C*). As expected, Tyrosine Hydroxylase (TH) immunolabeling was decreased in particular areas, e.g., the striatum (Fig. 3 *C*, *a* and *b*). In the anterior cingulate cortex (ACC), 6-OHDA injection only modified the TH-labeled area (Fig. 3 *C*, *e* and *f*) but not the labeling intensity. In contrast, no variations of TH immunostaining were detected in hypothalamic nuclei, including the hypothalamic A11 area projecting to the spinal cord (34) (Fig. 3 *C*, *c* and *d*). Accordingly, no changes were observed in the TH innervation of the dorsal spinal cord (Fig. 3 *C*, *g* and *h*). Desipramine pretreatment protected noradrenergic fibers, and TH depletion was mainly seen in Dopamine Active Transporter (DAT)-positive, dopaminergic fibers (*SI Appendix*, Fig. S4). Because the majority of dopamine neurons form heterogeneous populations located in the midbrain areas (35), we used specific markers of these populations (36) and determined that vasoactive intestinal peptide (VIP)-containing TH fibers are more sensitive to the 6-OHDA lesion than Aldehyde dehydrogenase 1 family, member A1 (Aldh1a1)-positive fibers (*SI Appendix*, Fig. S5).

Finally, we analyzed the ERK1/2 MAP kinase and CaMKIIα intracellular signaling pathways involved in CREB activation (37) and spinal sensitization to inflammatory conditions (38, 39) by using Western blotting (Fig. 3*D*) and immunohistochemistry (Fig. 3*E*). Western blotting of the ipsilateral dorsal spinal cord revealed an increased expression of the excitatory marker CaMKIIα in 6-OHDA mice (Fig. 3*D*). Similarly, the labeling for the phosphorylated forms of ERK1/2 MAP kinase (pERK) and the CREB transcription factor (pCREB) (Fig. 3*D*) was significantly stronger in 6-OHDA mice. Immunolabeling for pERK

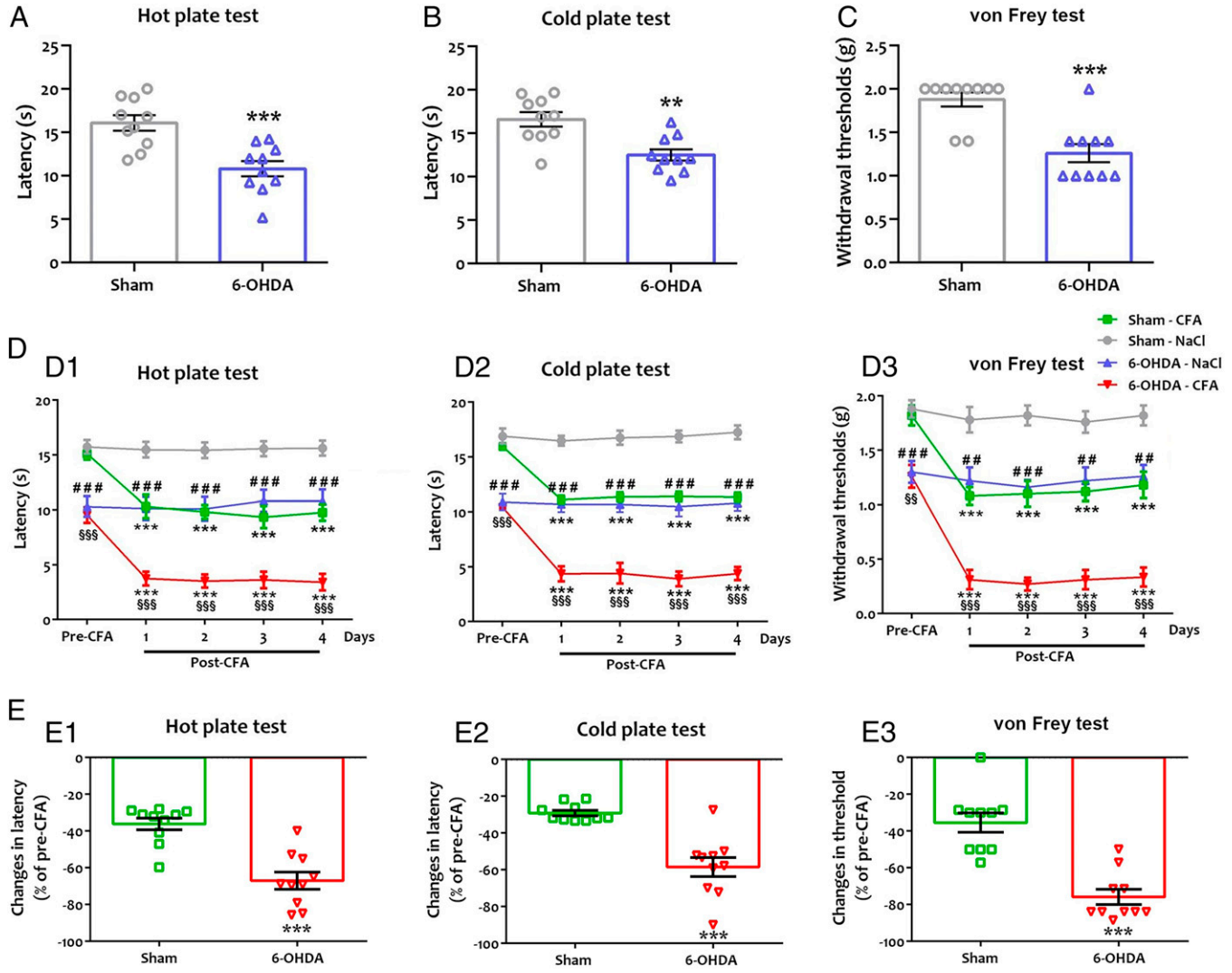

Fig. 1. Hypersensitivity to hot (*A*), cold (*B*) and mechanical (*C*) nociceptive stimuli in ADHD-like conditions, and after CFA injection (*D, E*). (*A*, *D1*, and *E1*) Paw-licking latency in hot plate (55 °C). (*B*, *D2*, and *E2*) Paw-licking latency in cold plate (5 °C). (*C*, *D3*, and *E3*) Paw withdrawal thresholds using von Frey filaments. (*A–C*) A significant decrease was found in paw-licking latency of 6-OHDA mice to hot (*A*, 10.81 ± 0.89 s vs. 16.07 ± 0.90 s; t = 4.16, *P* = 0.0006) and cold (*B*, 12.51 ± 0.66 s vs. 16.60 ± 0.83 s; t = 3.87, *P* = 0.002) stimuli and in paw withdrawal from mechanical stimulus (*C*, 1.26 ± 0.10 g vs. 1.88 ± 0.08 g; t = 4.74, *P* = 0.0002), in comparison to sham mice. All data are means ± SEM (10 mice per group), $^{**}P < 0.01$; $^{***}P < 0.001$ vs. sham. (*D1–D3*) We evaluated ADHD-induced sensitization under inflammatory conditions. After the pretest (1 d before CFA injection; pre-CFA), CFA or saline was injected in the sole of the right hind paw. The post-test (post-CFA) was done 4 d after CFA injection. A 2-way repeated-measures ANOVA showed a significant effect of the lesion (6-OHDA) ([heat]: $F_{(3,27)} = 98.48$, *P* = 0.0001; [cold]: $F_{(3,27)} = 257.0$, *P* = 0.0001; [von Frey]: $F_{(3,27)} = 243.4$, *P* = 0.0001), inflammation (CFA) ([heat]: $F_{(4,36)} = 9.69$; *P* = 0.0001; [cold]: $F_{(4,36)} = 14.64$, *P* = 0.0001; [von Frey]: $F_{(4,36)} = 20.40$, *P* = 0.0001), and interaction 6-OHDA × CFA ([heat]: $F_{(12,108)} = 3.62$, *P* = 0.0001; [cold]: $F_{(12,108)} = 5.47$, *P* = 0.0001; [von Frey]: $F_{(12,108)} = 3.60$, *P* = 0.0002) on thermal and mechanical sensitivity. There was a significant decrease in licking latency to thermal stimuli in sham mice ([heat]: 9.77 ± 0.75 s vs. 15.11 ± 0.54 s; q = 6.87, *P* = 0.0001; [cold]: 11.33 ± 0.41 s vs. 15.95 ± 0.29 s; q = 7.72, *P* = 0.0001) and 6-OHDA mice ([heat]: 3.42 ± 0.75 s vs. 9.53 ± 0.72 s; q = 7.86, *P* = 0.0001; [cold]: 4.38 ± 0.59 s vs. 10.43 ± 0.13 s; q = 10.11, *P* = 0.0001) 4 d post-CFA in comparison to the pre-CFA. CFA injection also resulted in a lowering of the mechanical threshold in sham mice (1.18 ± 0.12 g vs. 1.82 ± 0.09 g; q = 6.12, *P* = 0.0001) and 6-OHDA mice (0.34 ± 0.09 g vs. 1.26 ± 0.10 g; q = 8.87, *P* = 0.0001) 4 d post-CFA in comparison to the pre-CFA. In contrast, intraplantar injection of NaCl in the hind paw had no effect on thermal sensitivity (sham: [heat]: 15.62 ± 0.70 s vs. 15.73 ± 0.63 s; q = 0.15, *P* > 0.05; [cold]: 17.24 ± 0.64 s vs. 16.89 ± 0.71 s; q = 0.59, *P* > *0.05*; 6-OHDA: [heat]: 10.80 ± 1.05 s vs. 10.31 ± 0.93 s; q = 0.63, *P* > 0.05; [cold]: 10.81 ± 0.71 s vs. 10.90 ± 0.74 s; q = 0.16, *P* > 0.05) and mechanical sensitivity (sham: 1.82 ± 0.09 g vs. 1.88 ± 0.08 g; q = 0.57, *P* > 0.05; 6-OHDA: 1.26 ± 0.10 g vs. 1.30 ± 0.10 g; q = 0.38, *P* > *0.05*) in both groups. All data are means ± SEM (10 mice per group), $^{***}P < 0.001$ vs. pre-CFA; $^{\#\#}P < 0.01$; $^{\#\#\#}P < 0.001$ vs. NaCl; $^{\S\S}P < 0.01$; $^{\S\S\S}P < 0.001$ vs. sham CFA. (*E1–E3*) Amplitude of changes in latency (*E1*, hot plate; *E2*, cold plate) or threshold (*E3*, von Frey). ADHD-like conditions increased CFA-induced sensitization in response to thermal ([heat]: −67.01 ± 4.60% vs. −36.20 ± 3.21%; t = 10.44, *P* = 0.0001; [cold]: −58.48 ± 5.22% vs. −29.12 ± 1.49%; t = 6.92, *P* = 0.0001) and mechanical (−75.86 ± 4.15% vs. −35.43 ± 5.32%; t = 12.19, *P* = 0.0001) stimuli. All data are mean percentage of pre-CFA ± SEM (10 mice per group), $^{**}P < 0.01$; $^{***}P < 0.001$ vs. sham.

(Fig. 3*E*) confirmed the increased expression levels of the phosphorylated kinase in the ipsilateral dorsal horn of 6-OHDA mice.

Inflammatory Status Influences ADHD-Like Symptoms. We determined whether nociceptive conditions influenced locomotor activity, anxiety, attention, and impulsivity in mice with inflammation (*SI Appendix*, Fig. S6 and Dataset S5). CFA injection decreased the distance traveled (*SI Appendix*, Fig. S6 *A1* and *A2*), mean mobility time (*SI Appendix*, Fig. S6*A3*), and velocity (*SI Appendix*, Fig. S6*A4*) of sham and 6-OHDA mice in the open-field test. Notably, CFA amplified 6-OHDA–induced hyperactivity. Indeed, the difference in distance traveled (*SI Appendix*, Fig. S6*A5*) and velocity (*SI Appendix*, Fig. S6*A7*) between the sham and 6-OHDA groups was higher in CFA conditions than after NaCl injection. Next, we evaluated anxiety-like behavior, a reported ADHD comorbidity, by using the elevated plus maze test, which has been recently validated to assess anxiety-like behavior in CFA mice (40). CFA injection decreased the time

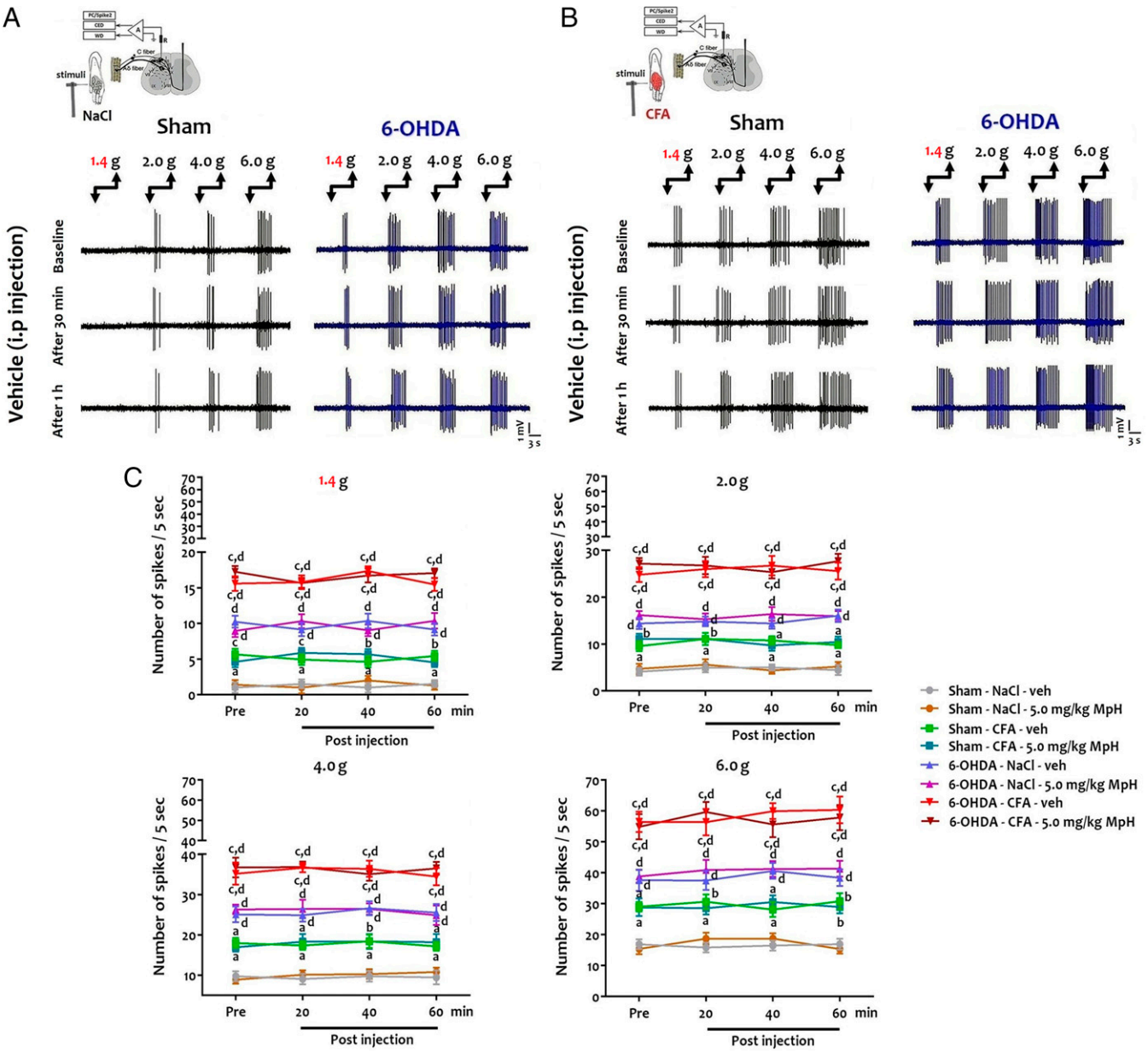

Fig. 2. Hyperexcitability of deep DHNs in ADHD-like conditions. (*A* and *B*) Single-unit in vivo extracellular recordings of deep DHNs in response to peripheral mechanical stimulation (1.4–6.0 g von Frey filament) under control (NaCl) and inflammatory conditions (CFA). (*C*) Quantification of the number of action potentials (number of spikes/5 s) after peripheral mechanical stimulation. Two-way repeated-measures ANOVA showed a significant effect of the group ([1.4 g]: $F_{(7,63)} = 207.7$, $P = 0.0001$; [2.0 g]: $F_{(7,63)} = 184.3$, $P = 0.0001$; [4.0 g]: $F_{(7,63)} = 159.0$, $P = 0.0001$; [6.0 g]: $F_{(7,63)} = 108.5$, $P = 0.0001$) on DHN electrical discharges. In contrast, Mph treatment (5.0 mg/kg Mph) ([1.4 g]: $F_{(3,27)} = 0.13$; $P = 0.094$; [2.0 g]: $F_{(3,27)} = 0.20$, $P = 0.90$; [4.0 g]: $F_{(3,27)} = 0.21$; $P = 0.89$; [6.0 g]: $F_{(3,27)} = 0.63$, $P = 0.60$) and interaction group × Mph ([1.4 g]: $F_{(21,189)} = 0.85$, $P = 0.66$; [2.0 g]: $F_{(21,189)} = 0.34$, $P = 0.99$; [4.0 g]: $F_{(21,189)} = 0.20$, $P = 0.99$; [6.0 g]: $F_{(21,189)} = 0.29$, $P = 0.099$) had no effect. There was a significant increase in the discharge of 6-OHDA mouse DHNs in response to innocuous ([1.4 g]: 10.25 ± 0.83 vs. 1.0 ± 0.73; q = 12.73, $P = 0.0001$) and noxious stimuli ([6.0 g]: 37.63 ± 3.42 vs. 16.88 ± 1.57; q = 7.77, $P = 0.0001$) in comparison to sham mice. In inflammatory conditions, there was a significant increase of DHN activity in response to innocuous ([1.4 g]: 5.67 ± 0.79 vs. 1.00 ± 0.73; q = 6.43, $P = 0.001$) and noxious stimuli ([6.0 g]: 29.02 ± 1.56 vs. 16.88 ± 1.57; q = 4.54, $P < 0.05$) in sham mice as compared to their controls (NaCl-injected sham mice). In contrast, CFA injection caused a further increase of DHN activity in 6-OHDA mice in response to both innocuous ([1.4 g]: 15.60 ± 1.03 vs. 10.25 ± 0.83; q = 7.36, $P = 0.0001$) and noxious stimuli ([6.0 g]: 56.49 ± 3.30 vs. 37.63 ± 3.42; q = 7.06, $P = 0.0001$) as compared to their controls (NaCl-injected 6-OHDA mice). After recording the baseline electrical activity of DHNs, Mph or vehicle (veh; 0.9% NaCl) was injected intraperitoneally and the single-unit extracellular recording was done every 20 min postinjection for 1 h. There was no significant effect of ADHD medication on electrical DHN activity in both the sham and 6-OHDA groups in response to peripheral innocuous and noxious mechanical stimulation under control (sham: [1.4 g]: 1.41 ± 0.65 vs. 1.28 ± 0.57; q = 0.18, $P > 0.05$; [6.0 g]: 15.42 ± 1.77 vs. 15.37 ± 1.49; q = 0.02, $P > 0.05$; 6-OHDA: [1.4 g]: 8.96 ± 0.87 vs. 10.38 ± 1.07; q = 1.95, $P > 0.05$; [6.0 g]: 38.84 ± 2.07 vs. 41.33 ± 2.55; q = 0.93, $P > 0.05$) and inflammatory conditions (sham: [1.4 g]: 4.63 ± 0.76 vs. 4.55 ± 0.64; q = 0.11, $P > 0.05$; [6.0 g]: 28.86 ± 2.80 vs. 28.97 ± 2.07; q = 0.04, $P > 0.05$; 6-OHDA: [1.4 g]: 28.86 ± 2.81 vs. 28.97 ± 2.08; q = 0.26, $P > 0.05$; [6.0 g]: 54.90 ± 4.08 vs. 57.87 ± 4.07; q = 1.11, $P > 0.05$). In addition, vehicle injection had no effect on DHN discharge in response to peripheral innocuous and noxious mechanical stimulation under control and inflammatory conditions in both sham and 6-OHDA groups. All data are means ± SEM (10 neurons per group), $^{a}P < 0.05$; $^{b}P < 0.01$; $^{c}P < 0.001$ vs. NaCl; $^{d}P < 0.001$ vs. sham.

spent and the number of entries in the open arms of the elevated plus maze in the sham and 6-OHDA groups (*SI Appendix*, Fig. S6 *B1–B3*). Therefore, anxiety-like behavior caused by ADHD-like conditions (30) was further worsened by the CFA treatment. The 6-OHDA–induced decrease in the time spent in the open arms of the elevated plus maze was amplified in CFA conditions as compared to the NaCl group (*SI Appendix*, Fig. S6*B4*). We performed the 5-choice serial reaction time task test to analyze

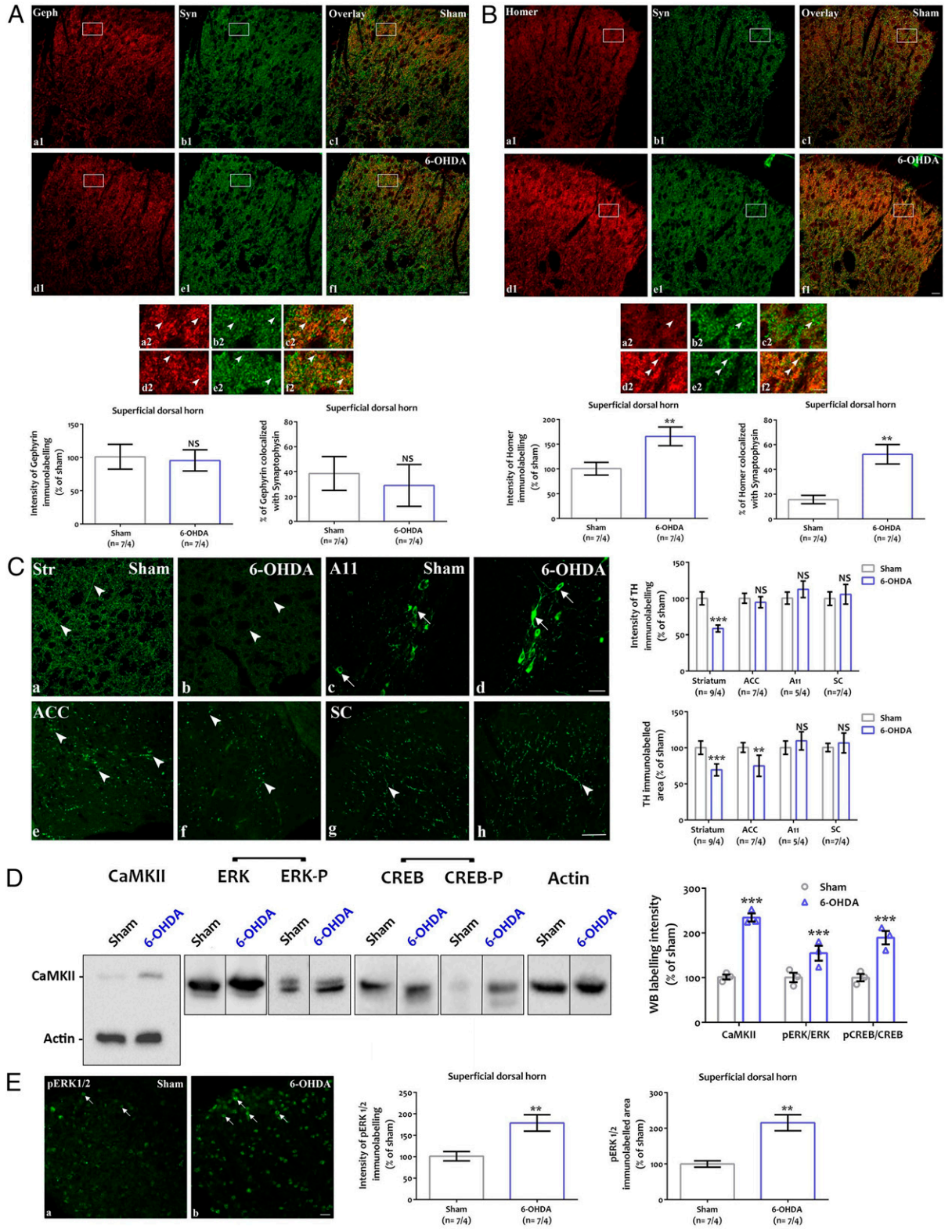

Fig. 3. ADHD-like conditions modify dorsal spinal networks. (*A* and *B*) Expression of synaptic markers in the dorsal spinal cord. Coexpression of postsynaptic gephyrin (*A*, red; *a1*, *d1*, *c1*, *f1*) or homer 1 (*B*, red; *a1*, *d1*, *c1*, *f1*) and presynaptic synaptophysin (*A* and *B*, green; *b1*, *c1*, *e1*, *f1*) in the dorsal horn of sham and 6-OHDA mice. Frames in *A*, *a1–f1* and *B*, *a1–f1* are displayed at higher magnification in *A*, *a2–f2* and B, *a2–f2*. Arrowheads point to close apposition between markers in *A*, *a2–f2* and *B*, *a2–f2*. Quantification of postsynaptic immunolabeling intensity (*Left*) and colocalization with the presynaptic marker synaptophysin (*Right*) shown in *A* and *B*. Homer 1, but not gephyrin, is overexpressed at synaptic sites in 6-OHDA mice ($n = 7$ sections in 4 mice; *t* test, *A*: $P > 0.05$; *B*: intensity: $^{**}P < 0.01$, $P = 0.0056$; colocalization: $P = 0.0019$) (Scale bar, 50 μm [*a1–f1*], 20 μm [*a2–f2*]). Geph: gephyrin, NS: nonsignificant, Syn: synaptophysin. (*C*) TH immunodetection of fibers (arrowheads) or cell bodies (arrows) in adult sham (*a*, *c*, *e*, *g*) and 6-OHDA (*b*, *d*, *f*, *h*) mice in the striatum (*a*, *b*), the A11 hypothalamic area (*c*, *d*), the ACC (*e*, *f*) and the spinal cord (*g*, *h*). The quantification shows that TH intensity is lowered in the striatum but not in the other areas, while the TH immunolabeled area is decreased in the striatum and ACC but is not affected in the A11 or the spinal cord ($n = 9$ [striatum], 7 [ACC and spinal cord], or 5 [A11] sections in 4 mice; *t* test, intensity in the striatum: $P = 0.000028$; area in the striatum: $P < 0.00001$; area in the ACC: $P = 0.0048$) (Scale bar, 50 μm). ACC: anterior cingulate cortex, NS: nonsignificant, SC: spinal cord, Str: striatum. $^{**}P < 0.01$, $^{***}P < 0.001$. (*D*) Western blotting detection of CaMKIIα, and total and phosphorylated forms of activation-dependent intracellular kinases (ERK) and transcription factor (CREB). CaMKII, pERK, and pCREB are overexpressed in 6-OHDA mice ($n = 4$ mice; *t* test, $^{***}P < 0.0001$, CaMKIIα: $P = 0.00086$; pERK/ERK: $P = 0.0063$; pCREB/CREB: $P = 0.00072$). (*E*) Immunodetection of pERK (arrows) in the dorsal horn of sham (*a*) and 6-OHDA (*b*) mice. The quantification of pERK labeling intensity and area indicates ERK activation in 6-OHDA mice ($n = 7$ sections in 4 mice; *t* test, $^{**}P < 0.01$, intensity: $P = 0.0057$, area: $P = 0.0069$) (Scale bar, 25 μm).

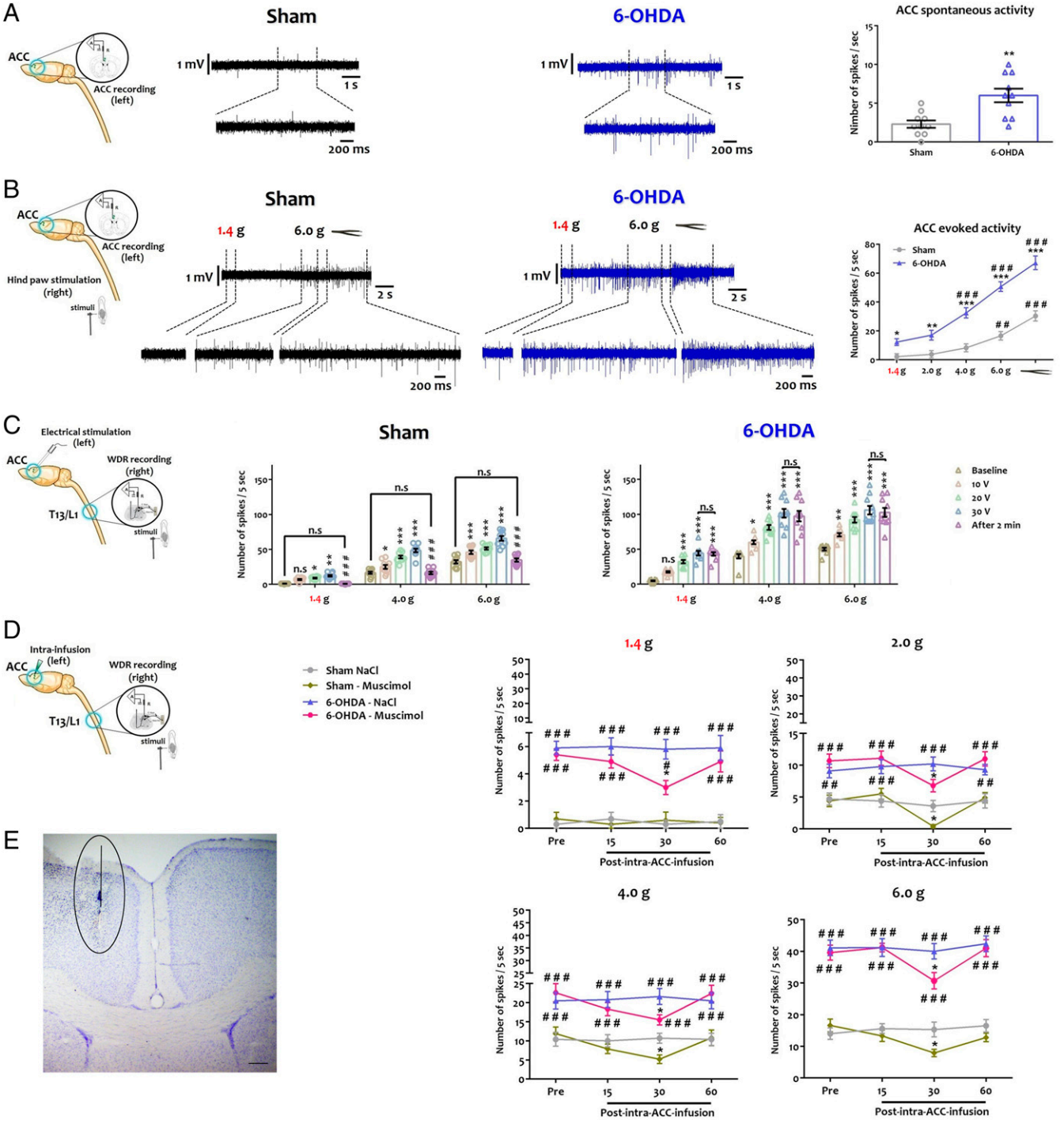

Fig. 4. The ACC is a key brain area of descending regulatory dysfunction in ADHD-like conditions. (*A*) From left to right: Representative diagram of the in vivo recording procedure of ACC neuron spontaneous activity. Single-unit in vivo extracellular recording of spontaneous activity of ACC neuron. Quantification of the number of action potential measured per second (see *SI Appendix*). $^{**}P < 0.01$ vs. sham. (*B*) From left to right: Representative diagram of the in vivo recording procedure of ACC neuron evoked activity. Single-unit extracellular recording of evoked activity recording of ACC neuron. Quantification of the number of action potential measured per 5 s upon peripheral mechanical stimulus of the hind paw, contralateral to the recorded ACC (von Frey filament: 1.4 g, 2.0 g, 4.0 g, 6.0 g, and pressure) (see *SI Appendix*). $^{*}P < 0.05$; $^{**}P < 0.01$; $^{***}P < 0.001$ vs. sham; $^{\#\#}P < 0.01$; $^{\#\#\#}P < 0.001$ vs. 1.4 g. (*C*) From left to right: Representative diagram of contralateral DHN neuron recording upon ACC electrical stimulation in response to different peripheral mechanical stimuli. Quantification of the number of action potentials per 5 s upon peripheral stimulus (von Frey filament: 1.4 g, 2.0 g, 4.0 g, 6.0 g) at different ACC electrical stimulation intensities (100 Hz: 10 V, 20 V, 30 V), and after 2 min of recovery (see *SI Appendix*). $^{*}P < 0.05$ vs. preinfusion; $^{\#\#\#}P < 0.001$ vs. sham. T13: thoracic vertebrae 13, L1: lumbar vertebrae 1. (*D*) From left to right: Representative diagram of contralateral DHN neuron recording upon ACC inhibition in responses to different peripheral mechanical stimuli. Quantification of the number of action potentials per 5 s upon peripheral stimulus (von Frey filament: 1.4 g, 2.0 g, 4.0 g, 6.0 g), every 15 min before and 1 h after muscimol infusion in the ACC (see *SI Appendix*). $^{*}P < 0.05$ vs Pre-infusion; $^{\#}P < 0.05$, $^{\#\#}P < 0.01$, $^{\#\#\#}P < 0.001$ vs Sham T13: thoracic vertebrae 13, L1: lumbar vertebrae 1. (*E*) Histological verification of the infusion site in the ACC. All data are means ± SEM (10 neurons per group).

inattention and impulsivity (*SI Appendix*, Fig. S6*C*). Inflammatory conditions did not affect inattention or impulsivity. Notably, no locomotor deficits were observed in CFA mice, which was further confirmed by the lack of differences in premature responses and perseverations. Taken together, these data suggest that inflammatory conditions worsen some of the ADHD-related

symptoms including hyperactivity and anxiety, but not impulsive-like behavior or inattention.

The ACC Is Involved in Nociception Control Dysfunctions in ADHD-Like Conditions. The ACC is central to both pain and ADHD disorders (27, 28) and sends projections to the dorsal horn of the spinal cord (41). Therefore, we tested the hypothesis that the ACC is responsible for the alteration of spinal circuits and nociceptive behavior in 6-OHDA mice (Fig. 4 and Dataset S6). We recorded ACC spontaneous (Fig. 4*A*) and evoked (Fig. 4*B*) activity in urethane-anesthetized animals. In vivo recordings indicated that ACC neurons were hyperactive in 6-OHDA mice (Fig. 4*A*), with higher action potential frequencies (Fig. 4*A*). Evoked activity was generated by applying mechanical stimuli on the posterior hind paw contralateral to the recorded ACC. Mechanical stimuli caused a stronger activity in the ACC of 6-OHDA animals as compared to sham animals when subjected to innocuous or noxious stimuli (Fig. 4 *B*). These observations suggested that the ACC hyperactivation seen in 6-OHDA mice may contribute to the altered sensory processing in the dorsal spinal cord.

We then explored the effects of ACC modulation on the activity of DHNs. First, we analyzed the effect of ACC activation on contralateral spinal cord responses evoked by peripheral mechanical stimuli (Fig. 4*C*). In vivo recording showed that the electrical stimulation (100 Hz) of ACC at different intensities increased contralateral DHNs activity in the sham group, in response to peripheral innocuous and noxious mechanical stimuli (Fig. 4*C*). This effect was significantly greater in 6-OHDA mice (Fig. 4*C*). Interestingly, spinal neuron activity returned to baseline activity within 2 min after the last electrical stimulation in sham mice, whether the stimulus was noxious or not, while the potentiation of spinal neuron activity in 6-OHDA mice was maintained up to 2 min (Fig. 4*C*). Next, we evaluated the effect of pharmacological inhibition of ACC by local muscimol injection to potentiate GABA-A inhibition (Fig. 4*D*). Muscimol partially blocked the electrical activity of contralateral DHNs in the sham and 6-OHDA groups, in response to peripheral mechanical stimuli, at 30 min after the drug injection (Fig. 4*D*). The proper location of the stimulation/injection site in ACC was confirmed histologically (Fig. 4*E*). Collectively, these data demonstrated that the heightened ACC activity in 6-OHDA mice makes a major contribution to the impairment of spinal sensory integration in ADHD conditions.

To confirm the role of ACC in nociception in 6-OHDA mice and identify the neuronal subtypes and their targets, we used optogenetics to activate or inhibit 1) excitatory neurons in the ACC or 2) their projection sites in the posterior insula (PI).

ACC Excitatory Neurons Amplify Nociceptive Sensitization in ADHD Conditions. We first injected $AAV_5.CamKII.ChR_2.eGFP$, $AAV_5.CamKII.ArchT_{3.0}.eGFP$, or $AAV_5.CamkII.eGFP$ unilaterally in the area 24b of the left ACC and illuminated the same area (*SI Appendix*, Fig. S7*A1*). The transduction efficiency was checked a posteriori by enhanced Green Fluorescent Protein (eGFP) visualization (*SI Appendix*, Fig. S7 *A2* and *A3*). The behavioral effects were displayed after stimulation of the paw contralateral (*SI Appendix*, Fig. S7) and ipsilateral (*SI Appendix*, Fig. S8) to the optogenetic manipulations. The effects on spinal neuron activity are shown only for the contralateral paw (*SI Appendix*, Fig. S7 and Dataset S7).

1. *Optogenetic activation.* At 4 wk after injection, ChR_2 activation induced a significant decrease in withdrawal thresholds to mechanical and thermal stimuli of the ipsilateral (left) (*SI Appendix*, Fig. S8*A1*) and contralateral (right) (*SI Appendix*, Fig. S7*B1*) hind paw of sham mice during the light phase. After the illumination period, the withdrawal thresholds returned to baseline values. Notably, the comparison of sham and 6-OHDA mice suggested that ADHD-like conditions amplified behavioral changes induced by light activation of ACC excitatory neurons in response to mechanical, but not thermal, stimulus to the contralateral paw (*SI Appendix*, Fig. S7*B2*). By contrast, no significant changes were seen in the ipsilateral paw whether mechanical or thermal stimulus (*SI Appendix*, Fig. S8*A2*) was applied.

We also evaluated DHN activity using in vivo single-unit recordings, contralateral to the adeno-associated virus (AAV) injection site in the ACC (*SI Appendix*, Fig. S7*C*). The results were in line with the behavioral tests. In sham and 6-OHDA animals, ACC optogenetic activation increased the activity of DHNs regarding mechanical stimuli (*SI Appendix*, Fig. S7*C*). After light activation, DHN activity decreased and returned to baseline levels (*SI Appendix*, Fig. S7*C*).

2. *Optogenetic inhibition.* Conversely, we silenced ACC excitatory neurons expressing $AAV_5.CaMKII.ArchT_{3.0}.eGFP$ (*SI Appendix*, Fig. S7*D*; see also *SI Appendix*, Fig. S8*B*). Optogenetic inhibition of ACC neurons had no significant effect on thresholds to mechanical or thermal stimuli of the ipsilateral (*SI Appendix*, Fig. S8*B1*) and contralateral paws (*SI Appendix*, Fig. S7*D1*) of sham animals. By contrast, we found that ACC neuron inhibition increased the mechanical threshold and withdrawal latency of 6-OHDA mice (*SI Appendix*, Figs. S7*D1* and S8*B1*). After illumination, both mechanical and thermal baseline sensitivity were fully restored. The comparison of sham and 6-OHDA mice indicated that ADHD-like conditions enhanced the analgesic effects induced by optogenetic inhibition of ACC excitatory neurons in response to mechanical stimulus of the contralateral hind paw (*SI Appendix*, Fig. S7*D2*). In contrast, no significant changes were seen in the ipsilateral hind paw whether thermal or mechanical stimulus (*SI Appendix*, Fig. S8*B2*) was applied.

In vivo recordings indicated no changes in the electrical activity of sham DHNs in response to stimuli when a light was on (*SI Appendix*, Fig. S7*E*). By contrast, ACC optogenetic inhibition significantly decreased DHN electrical activity in 6-OHDA mice (*SI Appendix*, Fig. S7*E*). After illumination, spinal neuron activity returned to the baseline levels (*SI Appendix*, Fig. S7*E*).

3. *Control experiments.* Sensory thresholds of ipsilateral (*SI Appendix*, Fig. S9*A2*) and contralateral paws (*SI Appendix*, Fig. S9*A1*) injected with the $AAV_5.CamKII.eGFP$ control virus were not affected by light stimulation in sham and 6-OHDA mice. Accordingly, illumination did not induce changes in spinal neuron activity after the transduction of $AAV_5.CamKII.eGFP$ (*SI Appendix*, Fig. S9 *B1* and *B2*).

The ACC–PI Excitatory Pathway Potentiates Nociceptive Sensitization in ADHD Conditions. We then sought to understand the circuit from the ACC to the spinal cord that is involved in ADHD-induced nociceptive sensitization. To manipulate the ACC–PI pathway, we used the same optogenetic strategy as previously described but placed the optical fiber in the ipsilateral PI (left side) (Fig. 5*A* and Dataset S8). Unilateral viral injection in the left 24b area (Fig. 5, *1* and 2) triggered virus expression in ACC fibers projecting to the ipsilateral PI (Fig. 5*A*, 3).

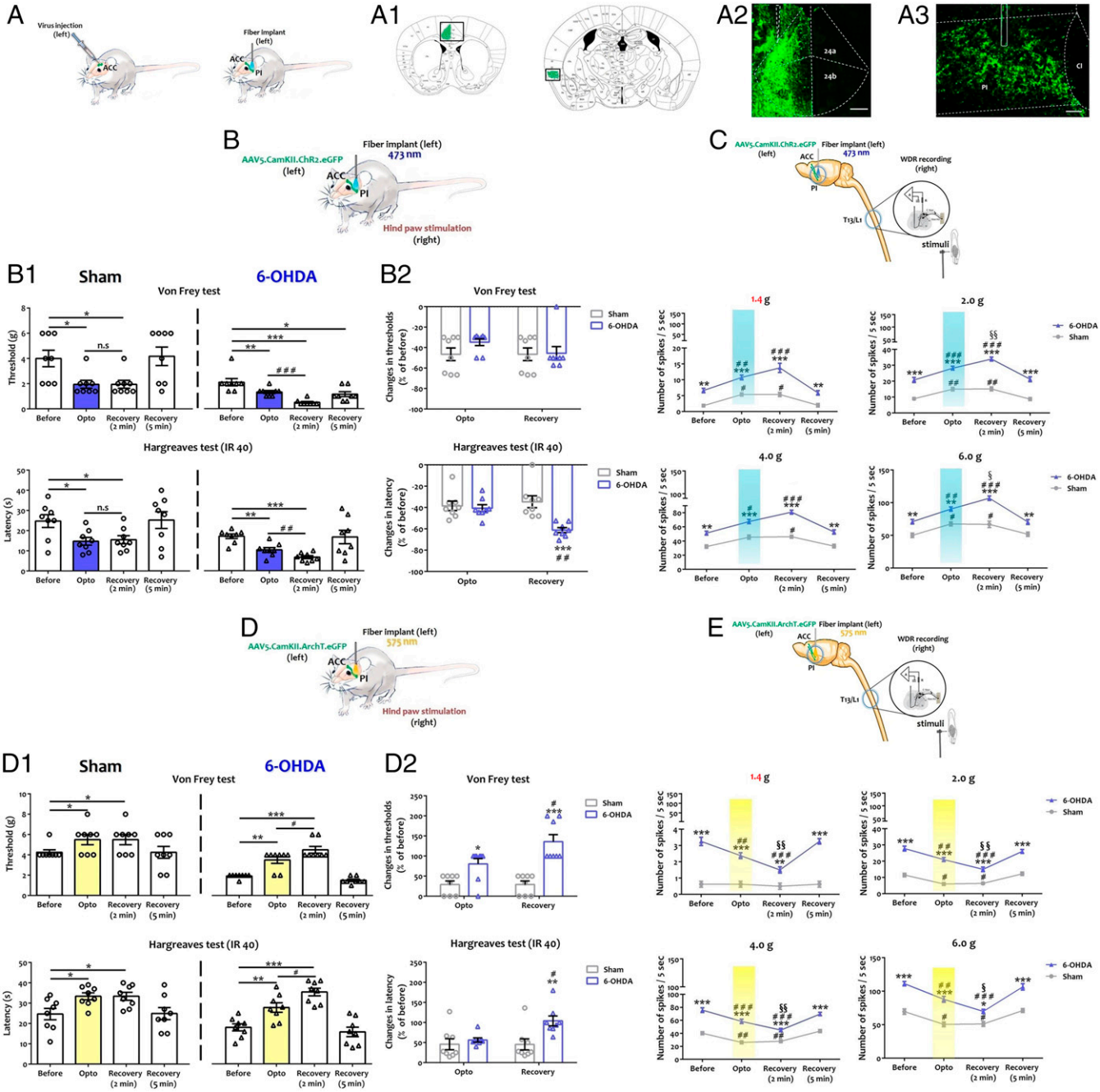

Fig. 5. Optogenetic modulation of the ACC–PI excitatory pathway potentiates sensitization of the contralateral paw in 6-OHDA mice. (*A*) Representative diagram of viral injection site in the left ACC (Left) and optic cannula placement (Right) in the left PI. (*A1*) Atlas representation of the ACC–PI pathway targeted in this study [Images modified from Paxinos and Franklin, 2001, with permission (42)]. (*A2* and *A3*) Examples of viral expression of ChR2-transduced ACC excitatory neurons (*A2*) projecting to the PI (*A3*). (Scale bar: ACC, 1 mm; PI, 200 μm.) (*B*) Activation of the left ACC–PI pathway in mice injected with AAV5.CaMKII.ChR2.eGFP and behavioral assessment on the contralateral (right) hind paw. (*B1*) von Frey and Hargreaves (infra-red radiant heat [40] 40) tests before (Before), during (Opto), and at 2 and 5 min after (Recovery) illumination (see *SI Appendix*). $^{*}P < 0.05$; $^{**}P < 0.01$; $^{***}P < 0.001$ vs. Before; $^{\#\#}P < 0.01$; $^{\#\#\#}P < 0.001$ vs. Opto. (*B2*) Amplitude of changes in withdrawal threshold and latency between Before and Opto or Recovery (2 min) conditions (% of values before illumination) (see *SI Appendix*). $^{***}P < 0.001$ vs. sham; $^{\#\#}P < 0.01$; vs. Opto. Circles: individual values for sham; triangles: individual values for 6-OHDA. (*C*) Activation of the left ACC–PI pathway of mice injected with AAV5.CaMKII.ChR2.eGFP and contralateral (right) DHN recording. Quantification of action potentials per 5 s upon peripheral stimulus before, during, and at 2 or 5 min after illumination (see *SI Appendix*). $^{**}P < 0.01$; $^{***}P < 0.001$ vs. sham; $^{\#}P < 0.05$; $^{\#\#}P < 0.01$; $^{\#\#\#}P < 0.001$ vs. Before; $^{\S}P < 0.05$ vs. Opto. (*D*) Silencing of the left ACC–PI pathway in mice injected with AAV5.CaMKII.ArchT.eGFP and behavioral assessment on the contralateral (right) hind paw. (*D1*) von Frey and Hargreaves tests before (Before), during (Opto), and at 2 or 5 min after (Recovery) illumination (see *SI Appendix*). $^{*}P < 0.05$; $^{**}P < 0.01$; $^{***}P < 0.001$ vs. Before; $^{\#}P < 0.05$ vs. Opto. (*D2*) Amplitude of changes in withdrawal threshold and latency between Before and Opto or Recovery (2 min) conditions (% of values before illumination) (see *SI Appendix*). $^{*}P < 0.05$; $^{**}P < 0.01$; $^{***}P < 0.001$ vs. sham; $^{\#}P < 0.05$ vs. Opto. Circles: individual values for sham; triangles: individual values for 6-OHDA. (*E*) Silencing of the left ACC–PI pathway in mice injected with AAV5.CaMKII.ArchT.eGFP and contralateral (right) DHN recording. Quantification of action potentials per 5 s upon peripheral stimulus before, during, and at 2 or 5 min after illumination (see *SI Appendix*). $^{*}P < 0.05$; $^{***}P < 0.001$ vs. sham; $^{\#}P < 0.05$; $^{\#\#}P < 0.01$; $^{\#\#\#}P < 0.001$ vs. Before; $^{\S}P < 0.05$; $^{\S\S}P < 0.01$ vs. Opto. All data are means ± SEM (8 neurons per group).

1. *Optogenetic activation.* In the sham group, the activation of *ChR*$_2$ resulted in a significant decrease in withdrawal thresholds to mechanical and thermal stimuli of the ipsilateral (*SI Appendix*, Fig. S10*A1*) and contralateral paws (Fig. 5*B*, *1* and Dataset S8). These changes were maintained until 2 min after the optogenetic stimulation was stopped and returned to

the preillumination baseline levels after 5 min. In 6-OHDA mice, withdrawal threshold or latency decreased significantly during illumination in response to thermal and mechanical stimuli. Interestingly, 2 min after optogenetic stimulation, the modification of mechanical and thermal thresholds was further amplified, which was not the case in sham mice. After 5 min, thermal thresholds returned to baseline levels, while the mechanical thresholds were not fully restored (Fig. 5*B*, *1* and *SI Appendix*, S10*A1*). Changes in paw withdrawal thresholds to thermal stimuli were stronger in ADHD-like conditions than in sham mice at 2 min recovery (Fig. 5*B*, *2* and *SI Appendix*, Fig. S10*A2* and Dataset S8).

In line with the behavioral data, in vivo recording in sham mice after ACC–PI pathway optogenetic activation revealed increased DHN activity after mechanical stimuli (Fig. 5*C* and Dataset S8). At 2 min after illumination, DHN activity remained unchanged and returned to the preillumination baseline levels after 5 min (Fig. 5*C*). In 6-OHDA mice, optogenetic activation of the ACC–PI excitatory pathway increased the activity of spinal neurons (Fig. 5*C*) that was further amplified at 2 min after illumination (Fig. 5*C*) and returned to the baseline levels at 5 min.

2. *Optogenetic inhibition.* Illumination of *Arch$T_{3.0}$* in the sham group resulted in a significant increase in thresholds to mechanical and thermal stimuli of the ipsilateral (*SI Appendix*, Fig. S10*B1*) and contralateral paws (Fig. 5*D*, *1* and Dataset S8). At 2 min after illumination, the increased thresholds were maintained and returned to baseline levels after 5 min. In 6-OHDA mice, the mechanical threshold and withdrawal latency of both the ipsilateral and contralateral hind paws increased significantly during illumination. Again, 2 min after the optogenetic inhibition ended, we found that both mechanical and thermal thresholds were further increased (Fig. 5*D*, *1* and *SI Appendix*, Fig. S10*B1*). The behavioral effects of optogenetic inhibition were amplified in 6-OHDA mice as compared to sham mice at 2 min recovery in response to both mechanical and thermal stimuli (Fig. 5*D*, *2* and Dataset S8) of the contralateral paw, while only in response to mechanical stimulus of the ipsilateral paw (*SI Appendix*, Fig. S10*B2*).

In vivo recordings (Fig. 5*E* and Dataset S8) revealed that optogenetic inhibition of the ACC – PI excitatory pathway in sham mice partially blocked the electrical activity of spinal neurons in response to noxious, but not innocuous, stimuli (Fig. 5*E*). Reduced DHN activity upon noxious stimuli was maintained at 2 min after illumination and returned to baseline levels after 5 min (Fig. 5*E*). In 6-OHDA mice, the optogenetic inhibition blocked the activity of spinal neurons in response to noxious and innocuous mechanical stimuli (Fig. 5*E*). In contrast to sham mice, spinal neuron activity in 6-OHDA mice was further decreased at 2 min after optogenetic inhibition ended (Fig. 5*E*).

3. *Control experiments.* In sham and 6-OHDA mice injected with the control virus, sensory thresholds were not affected by light stimulation whether for the ipsilateral (*SI Appendix*, Fig. S11*A2*) or contralateral (*SI Appendix*, Fig. S11*A1*) paw. In addition, in vivo recordings confirmed the absence of the light effect on spinal neurons in *AAV_5.CamkII.eGFP*-expressing sham or 6-OHDA mice (*SI Appendix*, Fig. S11 *B1* and *B2*).

Overall, these data indicated that ADHD-like conditions impaired the regulation exerted by the ACC–PI excitatory pathway on nociceptive behavior and spinal neuron activity in 6-OHDA mice.

Discussion

The present study reports hypersensitivity to mechanical, heat, and cold stimuli in a mouse model of ADHD obtained by postnatal disruption of dopaminergic systems. Under inflammatory conditions, the sensitization of withdrawal reflexes was further amplified in 6-OHDA mice. Behavioral changes were accompanied by the increased excitability of spinal neurons and changes in spinal networks. Physiological and behavioral alterations were correlated to ACC hyperactivity in 6-OHDA mice. Manipulating the ACC or the ACC–PI excitatory pathway had bidirectional effects on spinal neuron activity and withdrawal reflexes. These effects were significantly amplified in 6-OHDA mice, revealing an impaired tuning of nociceptive modulation processes in ADHD-like conditions.

Clinical studies in children with ADHD have described both hypo- and hyperresponsiveness to sensory stimuli (43, 44) and point to an increased prevalence of generalized pain in adults with ADHD as compared to a control population (15). In agreement with these findings, experimental studies have demonstrated changes in pain perception in patients with ADHD (12). Reciprocally, chronic pain increases impulsivity (26) and induces attentional and cognitive deficits in human patients (18, 19) and preclinical animal models (20, 45). Increased pain sensation in ADHD patients is thought to be caused by brain mechanisms leading to exacerbated perception. However, data also point to alterations in sensory transmission and reciprocal association between altered sensory processing and attention deficits (8).

Deregulation of the dopaminergic systems is involved in the etiology of ADHD in human and rodent models (23, 26). In addition, dopaminergic system dysfunctions in patients underpin the painful hypersensitivity observed in the context of fibromyalgia or restless legs syndrome (46) and in the genesis of chronic sensory alterations in rodents (47). Accordingly, many substances that increase dopaminergic transmission have analgesic properties (48). The neonatal 6-OHDA lesion in mice replicates the alterations of dopaminergic systems. This model has been validated by us (29, 30) and others (49–51) as a model of ADHD with good face, construct, and predictive validity. In the present study, we further confirmed that the 6-OHDA model exhibits the major symptoms of ADHD, i.e., hyperactivity, inattention, and impulsivity, as well as anxiety-like behavior. This combination of symptoms is a good hallmark of ADHD-like conditions. Other symptoms that have not been tested here were previously reported in the 6-OHDA model: impaired latent inhibition, selective attention, cognitive functions, and antisocial behavior (29, 30). Notably, this neonatal 6-OHDA model is different from the classical Parkinson's disease rodent model obtained by a 6-OHDA lesion of the medial forebrain bundle (52) or the substantia nigra (53) in adult mice. In particular, no signs of locomotor deficit were detected in our ADHD-like model.

A key finding of the present study is that nociceptive sensitization observed in 6-OHDA mice is supported by the impairment of sensory integration in the spinal cord, i.e., increase in excitatory contacts, hyperactivation of excitatory intracellular signaling pathways, and hyperexcitability of WDR spinal neurons. Electrophysiology data from DHNs suggest that increased sensitivity is caused by DHN hyperexcitability in the 6-OHDA model. The augmented activity of DHNs is a hallmark of central sensitization, leading to chronic sensory alterations in rodent models of chronic inflammatory (54) and neuropathic (39) pain. The present study indicates increased immunoreactivity for homer 1 at synaptic sites that has been also observed in inflammatory conditions (55) and

after nerve injury (56) in rodents. The long forms of homer are located in the postsynaptic density, and their up-regulation may result from an increase in the number and/or size of glutamatergic synapses (57). In addition, the accumulation of homer 1 is in agreement with the increased expression of other excitatory postsynaptic scaffolding proteins, e.g., shank or PSD95, in chronic pain–like conditions (58). In conjunction with increased excitability and excitatory synaptic connections, immunohistochemical and biochemical data in 6-OHDA mice reveal the activation of intracellular signaling pathways known to be involved in central sensitization to noxious stimuli (57, 58). Taken together, these data suggest increased excitation that may underlie spinal central sensitization processes (59) in the spinal cord of 6-OHDA mice.

The primary source of catecholaminergic innervation of the spinal cord is the A11 hypothalamic area (34). However, spinal circuits are not directly affected by the depletion in dopamine induced by postnatal 6-OHDA injection since TH immunoreactivity is not modified in the A11 area or in the dorsal spinal cord in 6-OHDA mice. Therefore, the modifications of spinal cord physiology in ADHD-like conditions, and their consequences for withdrawal reflexes, are likely caused by alterations of other brain circuits that engage descending pathways using various neurotransmitter systems. Indeed, serotonin/norepinephrine-mediated descending facilitation originating from the brainstem has been recently indicated to play key roles in central sensitization for nociceptive inputs and maintenance of chronic sensory disorders in different animal models (60).

Following the pioneering work of Reynolds (61), both inhibitory and facilitatory descending influences on spinal nociceptive processing have been widely studied in rodent models and humans (60, 62). However, most previous studies focused on descending modulation from the brainstem, and only recently has the role of cortical and subcortical structures been considered in the control of spinal neuron activity (63, 64) and nociceptive behavior in pathological conditions (65). ACC is an important cortical area with clinical relevance in patients with chronic pain (66). Neuroimaging studies in patients with ADHD identified structural and functional abnormalities in networks comprising the ACC and parietal cortices (67). Persistent pain-like conditions in rodents are characterized by the potentiation of synaptic responses (68), disinhibition (69), and increased excitability (70) of the ACC. Furthermore, ACC hyperactivity is a crucial link between pain and its comorbid emotional disorders (71). Contrary to other studies that described a role of rostral ACC in the negative affect and depression-like behavior associated with chronic pain but not mechanical hypersensitivity per se (71), our data were obtained in the dorsal part of the ACC and indicate that these areas actually control sensory transmission in the spinal cord. At a mechanistic level, future experiments will be required to determine the cellular and molecular mechanisms underpinning ACC dysfunction in ADHD-like conditions, and the possibility to engage cross-callosal projections (72) that may be responsible for the bilateral effect seen in our optogenetic experiments.

Taken together, these data provide a framework that strongly supports our findings of mutual interactions between ADHD-like conditions and sensory disorders. Postnatal injection of 6-OHDA in mice resulted in ACC hyperactivity in adulthood. The up- or down-regulation of ACC activity, and more particularly that of glutamatergic neurons, can increase or decrease, respectively, spinal neuron excitability and withdrawal reflex. This factor is in agreement with previous studies showing that persistently activated ACC neurons cause tonic potentiation of spinal sensory transmission and contribute to the maintenance of behavioral hyperalgesia (73). The insula receives inputs from the ACC and controls spinal networks and nociceptive behavior (65). It participates in nociceptive processing in rodents and humans (74, 75) and codes for pain intensity (76). Accordingly, we established that the ACC–PI excitatory pathway is impaired in ADHD-like conditions and bidirectionally modulates spinal neuron activity and withdrawal reflexes. Sensory gating by the ACC–PI pathway may engage the downstream recruitment of facilitatory descending serotoninergic projections, probably from the rostroventral medulla (RVM) to the spinal cord (65). In addition, patients with ADHD have displayed structural alterations of the insula, supporting a role for this structure in modulating attention and inhibitory capacity in ADHD (77).

The role of the ACC–PI excitatory circuit does not exclude the involvement of other, top-down pathways. This hypothesis is supported by the differences seen in mechanical or thermal sensitization depending on the manipulation of the ACC as a whole, or more specifically of the ACC–PI circuit, respectively. The latter may be responsible for the amplification of thermal sensitization, whereas other circuits could be implicated in mechanical sensitization. Previous studies demonstrated a direct, RVM-independent, ACC–spinal cord pathway, that facilitates the activity of laminae I–II spinal neurons and potentiates withdrawal reflexes (63). Future studies will be needed to assess the respective contribution of these different parallel top-down pathways, arising from the ACC, in the control of spinal networks in ADHD-like conditions. Whether modulation of the ACC–PI circuit also alters ADHD-like symptoms also remains to be established.

Mph is effective to relieve ADHD-related symptoms in humans (78) and mice (30). However, the administration of Mph did not alleviate allodynia and hyperalgesia in 6-OHDA mice. Therefore, nociception and ADHD-like symptoms are likely underpinned by partially different brain circuits. This was further confirmed by the observation that enhancing nociception with CFA had different consequences for the different ADHD-like symptoms. CFA-induced inflammatory conditions modified the hyperactivity and anxiety behavior of 6-OHDA mice. Surprisingly, modulating nociception had no effect on attention or impulsivity in this model. This finding is in contrast with several studies that have demonstrated tight links between pain and attentional states that also involve ACC and the insular cortex (10, 79). However, some findings point to the differential effects of pain on various attentional tasks (18). Notably, most studies to date have considered the effect of acute painful stimuli on attention, and only rarely have the consequences of chronic pain states been reported (19).

In a context of high prevalence of chronic pain (80) and ADHD (2) characterized by the ineffectiveness of currently available treatments, the present study provides insights into the understanding of cross-effects between these pathologies. ADHD and pain may be critically involved in regulating specific subcircuits originating from the ACC and underpinning spinal sensitization to nociceptive transmission and ADHD-like symptoms. An increased understanding of mechanisms that underlie the overlap of psychiatric disorders with pain are key factors in the development of new therapies.

Methods

Detailed *Methods* are available in *SI Appendix*. The different work flows are depicted in *SI Appendix*, Fig. S12.

Animal Models. The experimental protocols have been validated by the local ethics committee under number 13126C. Swiss mice received an intracerebroventricular injection of 6-OHDA or artificial cerebrospinal fluid aCSF at P5 (29, 30).

Inflammatory models of pain were obtained by CFA or NaCl injection in the hind paw. Mph or vehicle was administered intraperitoneally.

Behavioral Tests. Nociceptive tests were conducted to assess mechanical (von Frey test), hot (hot plate and plantar tests), and cold (cold plate) sensitization. Hyperactivity was measured with the open-field assay. Attention and impulsivity were assessed with the 5-choice serial reaction time task test, as previously described (29). The elevated plus maze was used to evaluate anxiety-like behavior.

In Vivo Electrophysiology. Single-unit in vivo recording of the ACC or spinal neurons was performed in anesthetized mice. In the dorsal horn, WDR neurons were identified as responding to noxious and innocuous stimuli. Recordings were then performed in response to the application of von Frey monofilaments with increasing bending forces on the hind paw, and action potential frequency was monitored. In the ACC, recording was also performed after local electrical activation or muscimol inhibition.

Optogenetics. ChR2 and ArchT3.0 opsin expression under the control of CaMKIIα promoter was driven in ACC excitatory neurons by local GFP-expressing AAV5 injection. Optical fibers were implanted in the ACC or the PI and excitation (blue light) or inhibition (yellow light) of ChR2 or ArchT3.0, respectively, was performed. The effects of optogenetic manipulation were assessed by measuring withdrawal reflexes and recording spinal neuron activity with in vivo electrophysiology.

Immunohistochemistry and Western Blotting. Synaptic markers (synaptophysin, homer 1, and gephyrin) were detected with immunofluorescence in the dorsal horn of sham and 6-OHDA mice. Labeling intensity and colocalization of homer 1 and gephyrin with synaptophysin were assessed quantitatively. TH immunoreactivity was detected in various brain areas and in the spinal cord. Markers of TH fibers (VIP, Aldh1a1, DAT, and Dopamine beta-hydroxylase (DBH)) were detected in the ACC. The expression of viral constructs was checked by GFP detection in the ACC and PI.

The activation of intracellular signaling pathways was assessed with Western blotting. Quantification was performed by normalizing the expression of markers (CaMKIIα, or pCREB and pERK1/2) to that of actin or nonphosphorylated proteins, respectively. pERK1/2 was also visualized by immunofluorescence in the dorsal horn.

Data Availability. All study data are included in the article and/or supporting information.

ACKNOWLEDGMENTS. This study was funded by a PHC Toubkal grant to M.B. and M.L. (Number TBK/15/20). O.B. was a recipient of a joint PhD scholarship (Campus France Number 32508PH). We thank the Mediterranean Neuroscience Society (https://www.medneuroscisociety.org/) for travel support. We are grateful to Thibault Dhellemmes and Marie Tuifua for technical help in immunohistochemical experiments. We thank Professor Åsa Mackenzie (Uppsala University) for valuable discussions about the subpopulations of TH-positive fibers. Imaging was performed at the Bordeaux Imaging Center, a member of the France BioImaging national infrastructure (ANR-10-INBS-04).

Author affiliations: [a]University of Bordeaux, CNRS, Interdisciplinary Institute for Neuroscience, UMR 5297, Bordeaux, France; [b]Laboratory of Pharmacology, Neurobiology, Anthropology & Environment, Faculty of Sciences, Cadi Ayyad University, Marrakesh, 40000, Morocco; [c]University of Bordeaux, CNRS, Institute of Neurodegenerative Diseases, UMR 5293, Bordeaux, France; and [d]University of Bordeaux, CNRS, INSERM, Bordeaux Imaging Center, UMS 3420, US 4, Bordeaux, France

1. J. Biederman, Attention-deficit/hyperactivity disorder: A selective overview. *Biol. Psychiatry* **57**, 1215–1220 (2005).
2. S. V. Faraone, J. Sergeant, C. Gillberg, J. Biederman, The worldwide prevalence of ADHD: Is it an American condition? *World Psychiatry* **2**, 104–113 (2003).
3. American Psychiatric Association, *Diagnostic and Statistical Manual of Mental Disorders* (American Psychiatric Association, Washington, DC, ed. 5, 2013).
4. J. J. Kooij *et al.*, Distinguishing comorbidity and successful management of adult ADHD. *J. Atten. Disord.* **16**, 3S–19S (2012).
5. D. B. Schatz, A. L. Rostain, ADHD with comorbid anxiety: A review of the current literature. *J. Atten. Disord.* **10**, 141–149 (2006).
6. L. Alexander, N. Farrelly, Attending to adult ADHD: A review of the neurobiology behind adult ADHD. *Ir. J. Psychol. Med.* **35**, 237–244 (2018).
7. A. R. Mao, R. L. Findling, Comorbidities in adult attention-deficit/hyperactivity disorder: A practical guide to diagnosis in primary care. *Postgrad. Med.* **126**, 42–51 (2014).
8. F. Dellapiazza *et al.*; for ELENA study group, Sensory processing related to attention in children with ASD, ADHD, or typical development: Results from the ELENA cohort. *Eur. Child Adolesc. Psychiatry* **30**, 283–291 (2021).
9. A. Kucyi, T. V. Salomons, K. D. Davis, Mind wandering away from pain dynamically engages antinociceptive and default mode brain networks. *Proc. Natl. Acad. Sci. U.S.A.* **110**, 18692–18697 (2013).
10. C. Villemure, C. M. Bushnell, Cognitive modulation of pain: How do attention and emotion influence pain processing? *Pain* **95**, 195–199 (2002).
11. A. B. M. Fuermaier *et al.*, Perception in attention deficit hyperactivity disorder. *Atten. Defic. Hyperact. Disord.* **10**, 21–47 (2018).
12. R. Treister, E. Eisenberg, N. Demeter, D. Pud, Alterations in pain response are partially reversed by methylphenidate (Ritalin) in adults with attention deficit hyperactivity disorder (ADHD). *Pain Pract.* **15**, 4–11 (2015).
13. C. Northover, A. Thapar, K. Langley, S. H. van Goozen, Pain sensitivity in adolescent males with attention-deficit/hyperactivity disorder: Testing for associations with conduct disorder and callous and unemotional traits. *PLoS One* **10**, e0134417 (2015).
14. A. Stickley, A. Koyanagi, H. Takahashi, Y. Kamio, ADHD symptoms and pain among adults in England. *Psychiatry Res.* **246**, 326–331 (2016).
15. L. L. Stray *et al.*, Motor regulation problems and pain in adults diagnosed with ADHD. *Behav. Brain Funct.* **9**, 18 (2013).
16. E. Vingilis *et al.*, Attention deficit hyperactivity disorder symptoms, comorbidities, substance use, and social outcomes among men and women in a Canadian sample. *BioMed Res. Int.* **2015**, 982072 (2015).
17. D. S. Veldhuijzen, J. L. Kenemans, C. M. de Bruin, B. Olivier, E. R. Volkerts, Pain and attention: Attentional disruption or distraction? *J. Pain* **7**, 11–20 (2006).
18. D. J. Moore, E. Keogh, C. Eccleston, The interruptive effect of pain on attention. *Q. J. Exp. Psychol. (Hove)* **65**, 565–586 (2012).
19. D. J. Moore *et al.*, The effect of induced and chronic pain on attention. *J. Pain* **20**, 1353–1361 (2019).
20. G. A. Higgins *et al.*, Enduring attentional deficits in rats treated with a peripheral nerve injury. *Behav. Brain Res.* **286**, 347–355 (2015).
21. M. Ogata, K. Noda, H. Akita, H. Ishibashi, Characterization of nociceptive response to chemical, mechanical, and thermal stimuli in adolescent rats with neonatal dopamine depletion. *Neuroscience* **289**, 43–55 (2015).
22. M. G. Liu, J. Chen, Preclinical research on pain comorbidity with affective disorders and cognitive deficits: Challenges and perspectives. *Prog. Neurobiol.* **116**, 13–32 (2014).
23. R. D. Oades *et al.*, The control of responsiveness in ADHD by catecholamines: Evidence for dopaminergic, noradrenergic and interactive roles. *Dev. Sci.* **8**, 122–131 (2005).
24. J. M. Swanson *et al.*, Etiologic subtypes of attention-deficit/hyperactivity disorder: Brain imaging, molecular genetic and environmental factors and the dopamine hypothesis. *Neuropsychol. Rev.* **17**, 39–59 (2007).
25. G. Tripp, J. R. Wickens, Neurobiology of ADHD. *Neuropharmacology* **57**, 579–589 (2009).
26. I. G. Ko *et al.*, Swimming exercise alleviates the symptoms of attention-deficit hyperactivity disorder in spontaneous hypertensive rats. *Mol. Med. Rep.* **8**, 393–400 (2013).
27. J. C. Bledsoe, M. Semrud-Clikeman, S. R. Pliszka, Anterior cingulate cortex and symptom severity in attention-deficit/hyperactivity disorder. *J. Abnorm. Psychol.* **122**, 558–565 (2013).
28. B. A. Vogt, Cingulate impairments in ADHD: Comorbidities, connections, and treatment. *Handb. Clin. Neurol.* **166**, 297–314 (2019).
29. O. Bouchatta, H. Manouze, S. Ba-M'Hamed, M. Landry, M. Bennis, Neonatal 6-OHDA lesion model in mouse induces cognitive dysfunctions of attention-deficit/hyperactivity disorder (ADHD) during young age. *Front. Behav. Neurosci.* **14**, 27 (2020).
30. O. Bouchatta *et al.*, Neonatal 6-OHDA lesion model in mouse induces attention-deficit/hyperactivity disorder (ADHD)-like behaviour. *Sci. Rep.* **8**, 15349 (2018).
31. C. Abboud *et al.*, Analgesic effect of central relaxin receptor activation on persistent inflammatory pain in mice: Behavioral and neurochemical data. *Pain Rep.* **6**, e937 (2021).
32. N. M. Elsherbiny *et al.*, Inhibitory effect of valproate sodium on pain behavior in diabetic mice involves suppression of spinal histone deacetylase 1 and inflammatory mediators. *Int. Immunopharmacol.* **70**, 16–27 (2019).
33. P. L. Foley, L. V. Kendall, P. V. Turner, Clinical management of pain in rodents. *Comp. Med.* **69**, 468–489 (2019).
34. K. Koblinger *et al.*, Characterization of A11 neurons projecting to the spinal cord of mice. *PLoS One* **9**, e109636 (2014).
35. A. Björklund, S. B. Dunnett, Dopamine neuron systems in the brain: An update. *Trends Neurosci.* **30**, 194–202 (2007).
36. J. F. Poulin, Z. Gaertner, O. A. Moreno-Ramos, R. Awatramani, Classification of midbrain dopamine neurons using single-cell gene expression profiling approaches. *Trends Neurosci.* **43**, 155–169 (2020).
37. A. E. West *et al.*, Calcium regulation of neuronal gene expression. *Proc. Natl. Acad. Sci. U.S.A.* **98**, 11024–11031 (2001).
38. C. J. Woolf, M. W. Salter, Neuronal plasticity: Increasing the gain in pain. *Science* **288**, 1765–1769 (2000).
39. P. Fossat *et al.*, Knockdown of L calcium channel subtypes: Differential effects in neuropathic pain. *J. Neurosci.* **30**, 1073–1085 (2010).
40. L. Luo *et al.*, Scopoletin ameliorates anxiety-like behaviors in complete Freund's adjuvant-induced mouse model. *Mol. Brain* **13**, 15 (2020).
41. A. A. Calejesan, S. J. Kim, M. Zhuo, Descending facilitatory modulation of a behavioral nociceptive response by stimulation in the adult rat anterior cingulate cortex. *Eur. J. Pain* **4**, 83–96 (2000).
42. G. Paxinos, K. B. J. Franklin, *The Mouse Brain in Stereotaxic Coordinates* (Academic Press, San Diego, CA, 2001).
43. H. L. Egger, E. J. Costello, A. Erkanli, A. Angold, Somatic complaints and psychopathology in children and adolescents: Stomach aches, musculoskeletal pains, and headaches. *J. Am. Acad. Child Adolesc. Psychiatry* **38**, 852–860 (1999).

44. N. Wolff *et al.*, Reduced pain perception in children and adolescents with ADHD is normalized by methylphenidate. *Child Adolesc. Psychiatry Ment. Health* **10**, 24 (2016).
45. M. Pais-Vieira, D. Lima, V. Galhardo, Sustained attention deficits in rats with chronic inflammatory pain. *Neurosci. Lett.* **463**, 98–102 (2009).
46. J. M. Jarcho, E. A. Mayer, Z. K. Jiang, N. A. Feier, E. D. London, Pain, affective symptoms, and cognitive deficits in patients with cerebral dopamine dysfunction. *Pain* **153**, 744–754 (2012).
47. T. Pelissier, C. Laurido, A. Hernandez, L. Constandil, A. Eschalier, Biphasic effect of apomorphine on rat nociception and effect of dopamine D2 receptor antagonists. *Eur. J. Pharmacol.* **546**, 40–47 (2006).
48. P. B. Wood, Role of central dopamine in pain and analgesia. *Expert Rev. Neurother.* **8**, 781–797 (2008).
49. E. Davids, K. Zhang, F. I. Tarazi, R. J. Baldessarini, Animal models of attention-deficit hyperactivity disorder. *Brain Res. Brain Res. Rev.* **42**, 1–21 (2003).
50. M. E. Avale *et al.*, The dopamine D4 receptor is essential for hyperactivity and impaired behavioral inhibition in a mouse model of attention deficit/hyperactivity disorder. *Mol. Psychiatry* **9**, 718–726 (2004).
51. A. Bari, T. W. Robbins, Animal models of ADHD. *Curr. Top. Behav. Neurosci.* **7**, 149–185 (2011).
52. R. Iancu, P. Mohapel, P. Brundin, G. Paul, Behavioral characterization of a unilateral 6-OHDA-lesion model of Parkinson's disease in mice. *Behav. Brain Res.* **162**, 1–10 (2005).
53. M. Lundblad, B. Picconi, H. Lindgren, M. A. Cenci, A model of L-DOPA-induced dyskinesia in 6-hydroxydopamine lesioned mice: Relation to motor and cellular parameters of nigrostriatal function. *Neurobiol. Dis.* **16**, 110–123 (2004).
54. M. Eliava *et al.*, A new population of parvocellular oxytocin neurons controlling magnocellular neuron activity and inflammatory pain processing. *Neuron* **89**, 1291–1304 (2016).
55. Y. X. Yao, Z. Jiang, Z. Q. Zhao, Knockdown of synaptic scaffolding protein Homer 1b/c attenuates secondary hyperalgesia induced by complete Freund's adjuvant in rats. *Anesth. Analg.* **113**, 1501–1508 (2011).
56. I. Obara *et al.*, Nerve injury-induced changes in Homer/glutamate receptor signaling contribute to the development and maintenance of neuropathic pain. *Pain* **154**, 1932–1945 (2013).
57. M. Gutierrez-Mecinas *et al.*, Immunostaining for Homer reveals the majority of excitatory synapses in laminae I-III of the mouse spinal dorsal horn. *Neuroscience* **329**, 171–181 (2016).
58. R. Kuner, Central mechanisms of pathological pain. *Nat. Med.* **16**, 1258–1266 (2010).
59. A. Latremoliere, C. J. Woolf, Central sensitization: A generator of pain hypersensitivity by central neural plasticity. *J. Pain* **10**, 895–926 (2009).
60. M. H. Ossipov, K. Morimura, F. Porreca, Descending pain modulation and chronification of pain. *Curr. Opin. Support. Palliat. Care* **8**, 143–151 (2014).
61. D. V. Reynolds, Surgery in the rat during electrical analgesia induced by focal brain stimulation. *Science* **164**, 444–445 (1969).
62. G. F. Gebhart, Descending modulation of pain. *Neurosci. Biobehav. Rev.* **27**, 729–737 (2004).
63. T. Chen *et al.*, Top-down descending facilitation of spinal sensory excitatory transmission from the anterior cingulate cortex. *Nat. Commun.* **9**, 1886 (2018).
64. O. Roca-Lapirot *et al.*, Acquisition of analgesic properties by the cholecystokinin/CCK2 receptor system within the amygdala in a persistent inflammatory pain condition. *Pain* **160**, 345–357 (2019).
65. L. L. Tan *et al.*, A pathway from midcingulate cortex to posterior insula gates nociceptive hypersensitivity. *Nat. Neurosci.* **20**, 1591–1601 (2017).
66. T. V. Bliss, G. L. Collingridge, B. K. Kaang, M. Zhuo, Synaptic plasticity in the anterior cingulate cortex in acute and chronic pain. *Nat. Rev. Neurosci.* **17**, 485–496 (2016).
67. N. C. Vetter *et al.*, Anterior insula hyperactivation in ADHD when faced with distracting negative stimuli. *Hum. Brain Mapp.* **39**, 2972–2986 (2018).
68. T. Chen *et al.*, Adenylyl cyclase subtype 1 is essential for late-phase long term potentiation and spatial propagation of synaptic responses in the anterior cingulate cortex of adult mice. *Mol. Pain* **10**, 65 (2014).
69. S. M. Blom, J. P. Pfister, M. Santello, W. Senn, T. Nevian, Nerve injury-induced neuropathic pain causes disinhibition of the anterior cingulate cortex. *J. Neurosci.* **34**, 5754–5764 (2014).
70. S. Cordeiro Matos, Z. Zhang, P. Séguéla, Peripheral neuropathy induces HCN channel dysfunction in pyramidal neurons of the medial prefrontal cortex. *J. Neurosci.* **35**, 13244–13256 (2015).
71. J. Sellmeijer *et al.*, Hyperactivity of anterior cingulate cortex areas 24a/24b drives chronic pain-induced anxiodepressive-like consequences. *J. Neurosci.* **38**, 3102–3115 (2018).
72. S. W. Hu *et al.*, Contralateral projection of anterior cingulate cortex contributes to mirror-image pain. *J. Neurosci.* **41**, 9988–10003 (2021).
73. T. Chen *et al.*, Postsynaptic potentiation of corticospinal projecting neurons in the anterior cingulate cortex after nerve injury. *Mol. Pain* **10**, 33 (2014).
74. A. R. Burkey, E. Carstens, L. Jasmin, Dopamine reuptake inhibition in the rostral agranular insular cortex produces antinociception. *J. Neurosci.* **19**, 4169–4179 (1999).
75. R. Peyron, B. Laurent, L. García-Larrea, Functional imaging of brain responses to pain. A review and meta-analysis (2000). *Neurophysiol. Clin.* **30**, 263–288 (2000).
76. A. R. Segerdahl, M. Mezue, T. W. Okell, J. T. Farrar, I. Tracey, The dorsal posterior insula subserves a fundamental role in human pain. *Nat. Neurosci.* **18**, 499–500 (2015).
77. M. P. Lopez-Larson, J. B. King, J. Terry, E. C. McGlade, D. Yurgelun-Todd, Reduced insular volume in attention deficit hyperactivity disorder. *Psychiatry Res.* **204**, 32–39 (2012).
78. L. M. Jonkman *et al.*, Perceptual and response interference in children with attention-deficit hyperactivity disorder, and the effects of methylphenidate. *Psychophysiology* **36**, 419–429 (1999).
79. R. Peyron *et al.*, Haemodynamic brain responses to acute pain in humans: Sensory and attentional networks. *Brain* **122**, 1765–1780 (1999).
80. D. Bouhassira, M. Lantéri-Minet, N. Attal, B. Laurent, C. Touboul, Prevalence of chronic pain with neuropathic characteristics in the general population. *Pain* **136**, 380–387 (2008).